The Phytocannabinoid (−)-Cannabidiol Operates as a Complex, Differential Modulator of Human Hair Growth: Anti-Inflammatory Submicromolar versus Hair Growth Inhibitory Micromolar Effects

Journal of Investigative Dermatology (2020) **140,** 484–488; doi:10.1016/j.jid.2019.07.690

TO THE EDITOR

Most cases of excessive hair loss and unwanted hair growth (e.g., effluvium, alopecia, hirsutism, hypertrichosis) result in part from major disturbances in the cyclic transformation of hair follicles (HFs), namely in their switch from active growth and pigmented hair shaft production (anagen) to apoptosis-driven HF involution (catagen) (Oh et al., 2016; Paus and Cotsarelis, 1999). It is now clear that this switch is profoundly influenced by complex neuroendocrine pathways, which still await systematic therapeutic targeting (Paus et al., 2014).

In this context, the endocannabinoid system is of special interest (Maccarrone et al., 2015; Oláh and Bíró, 2017; Tóth et al., 2019). Specifically, activation of CB_1 receptors by the endocannabinoid anandamide, and the plant-derived (−)-Δ^9-*trans*-tetrahydrocannabinol, promotes premature catagen entry in human scalp HFs ex vivo (Telek et al., 2007). However, 2-arachidonoylglycerol, another prototypic endocannabinoid, does not modulate HF growth ex vivo, suggesting functional heterogeneity between different cannabinoids in terms of human hair growth modulation (Telek et al., 2007).

This motivated us to also explore how another phytocannabinoid, (−)-cannabidiol (CBD), impacts on human hair growth. This major non-psychotropic phytocannabinoid does not activate CB_1 receptors, but may context-dependently signal via modulating several other targets (e.g., GPR55, 5-HT_{1a}, or μ-opioid receptors) (Pertwee, 2008). Moreover, it is used in clinical practice in multiple sclerosis and certain epilepsies, and is currently under intense investigation for various uses in clinical medicine, ranging from neuropsychiatric disorders to acne (ID at ClinicalTrials.gov: NCT03573518) (Armstrong et al., 2015; Chelliah et al., 2018; Crippa et al., 2018; Esposito et al., 2013; Pisanti et al., 2017). In fact, CBD exerts complex sebostatic and anti-inflammatory effects on the pilosebaceous unit by activating both transient receptor potential vanilloid-4 (TRPV4) ion channels and adenosine A_{2A} receptors on sebocytes (Oláh et al., 2014). Topically administered CBD is likely to also reach human HFs, which express functional TRPV4 receptors, the stimulation of which induces premature catagen (Szabó et al., 2019), whereas adenosine reportedly promotes human hair growth (Oura et al., 2008).

Therefore, we asked in the current exploratory pilot study whether and how CBD impacts on microdissected, organ-cultured human scalp HFs (Langan et al., 2015) and primary human outer root sheath keratinocytes (ORSKs) isolated and cultured from plucked hair shafts (Ramot et al., 2018), obtained after written informed consent from dermatologically healthy individuals. The study adhered to Helsinki guidelines, and was institutionally and governmentally approved. For methodological details, see Supplementary Materials and Methods.

First, we probed if CBD influenced hair shaft production of microdissected human HFs. We found that, when applied at 0.1 μM, CBD tended to promote hair shaft elongation, but, unexpectedly, did not modulate HF cycling and hair matrix keratinocyte proliferation or apoptosis ex vivo (Figure 1). This tendency may represent a pseudo-elongation of the hair shaft, which is pushed out of its anchorage in the HF by tissue shrinkage during the course of organ culture. However, 10 μM CBD significantly suppressed hair shaft production (Figure 1a and Supplementary Figure S1), and induced development of catagen morphology (Figure 1b and c). This was accompanied by a significant reduction of the ratio of proliferating (Ki-67^+), and a significant increase in the percentage of apoptotic ($TUNEL^+$) hair matrix keratinocytes (Figure 1d and e), indicating the onset of an apoptosis-associated involution. This invited the hypothesis that CBD may concentration-dependently target different receptors.

This hypothesis was probed in cultured ORSKs, which facilitate mechanistic analyses and permit higher throughput assessments than very scarcely available scalp HFs. In line with the above HF data, CBD rapidly decreased the ORSK count (3- to 72-hour treatments; CyQUANT assay; Supplementary Figure S2a-d), reduced viability, and induced chiefly apoptotic cell death in a concentration- and time-dependent manner (24-hour treatments; MTT assay and combined 1,1′,3,3,3′,3′-hexamethylindodicarbocyanine iodide ($DilC_1(5)$)-SYTOX Green labeling; Supplementary Figure S3a and b).

CBD activates the mostly calcium-permeable TRPV4 ion channels (Oláh et al., 2014), the stimulation of which promotes catagen in human HFs ex vivo (Szabó et al., 2019). In line with this, the catagen-promoting CBD

Abbreviations: CBD, (−)-cannabidiol; HF, hair follicle; TLR, toll-like receptor; TRPV4, transient receptor potential vanilloid-4

Accepted manuscript published online 29 July 2019; corrected proof published online 15 October 2019

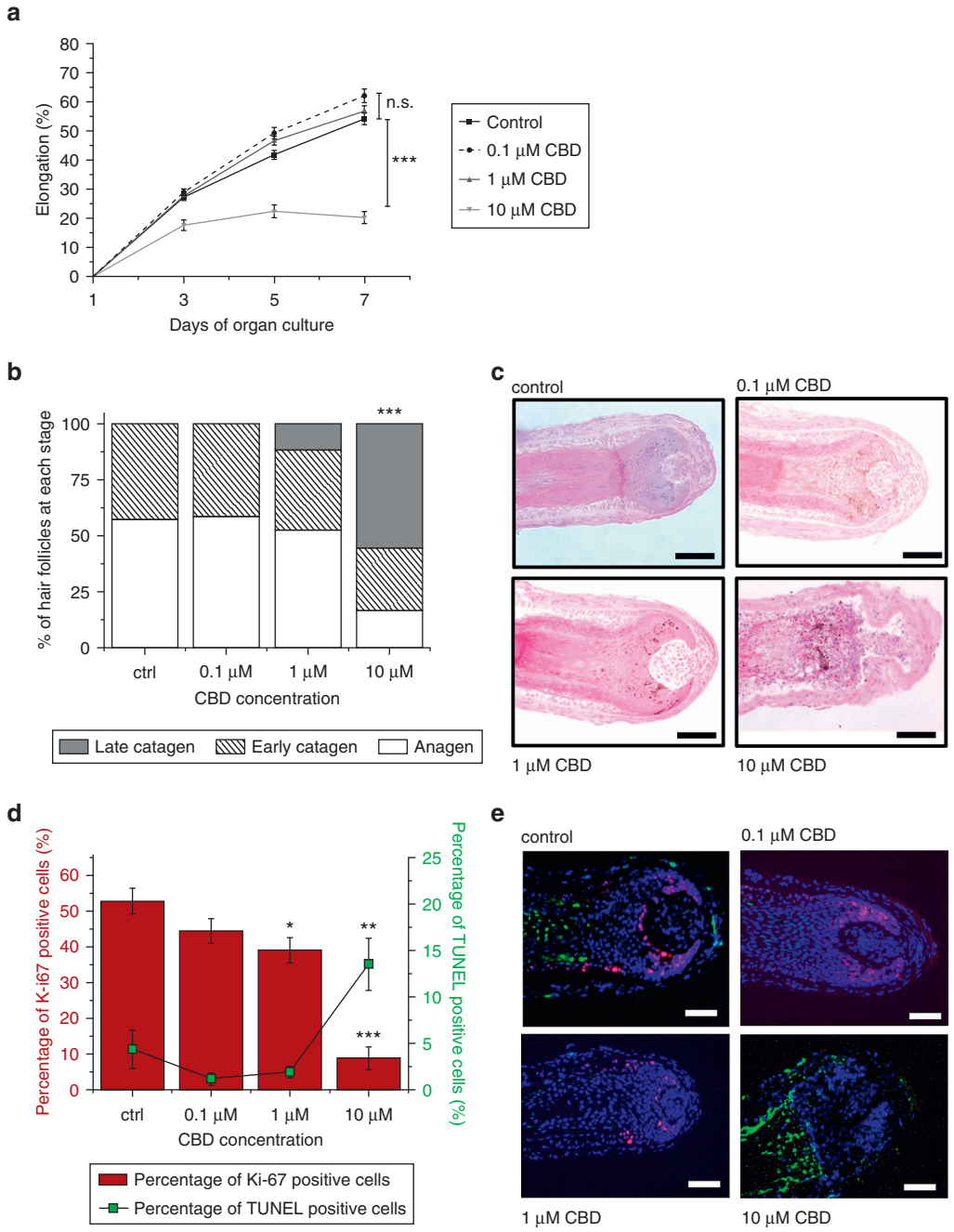

Figure 1. CBD differentially influences elongation as well as hair cycle of human microdissected HFs. (**a**) Hair shaft elongation curves. HFs (N = 54 HFs from three donors per treatment, expressed as mean ± standard error of the mean) were treated as indicated. ***$P < 0.001$, respectively, significant differences as indicated at day 7 (i.e., after 6 days of treatment). (**b**) Results of microscopic hair cycle staging. ***$P < 0.001$ significant differences (chi-square test followed by Fisher's exact test) compared with the control group. (**c**) Sections of representative HFs following hematoxylin and eosin staining. (**d**) Percentages of proliferating (Ki-67$^+$) and apoptotic (TUNEL$^+$) matrix keratinocytes were determined. Data are expressed as mean ± standard error of the mean of N = 36–40 HFs from three donors per treatment. *$P < 0.05$, **$P < 0.01$, and ***$P < 0.001$, respectively, significant differences compared with the respective control groups. (**e**) Representative pictures of Ki-67 (red) and TUNEL (green) double staining after the indicated treatments. Nuclei were counterstained by DAPI (blue). CBD, (−)-cannabidiol; HF, hair follicle. Bar = 50 μm.

concentration (≥10 μM) induced calcium influx in cultured ORSKs (Figure 2a and b), which was almost completely abrogated by the highly selective TRPV4 antagonist, HC067047 (1 μM) (Everaerts et al., 2010; Figure 2c and d). This suggests that, at micromolar concentrations, CBD activates TRPV4 in human ORSKs, and that its catagen-promoting effect on organ-cultured HFs may be stimulated via signaling through this newly identified catagen-inducing pathway.

Reportedly, toll-like receptor 3 activation on human ORSKs leads to inflammasome activation and subsequent IL-1β production (Shin et al., 2017), which may create a proinflammatory, catagen- and HF dystrophy-promoting signaling milieu (Hoffmann et al.,1998; Philpott et al., 1996; Rückert et al., 2000). Since CBD exerts remarkable anti-inflammatory effects in several systems (Esposito et al., 2013;

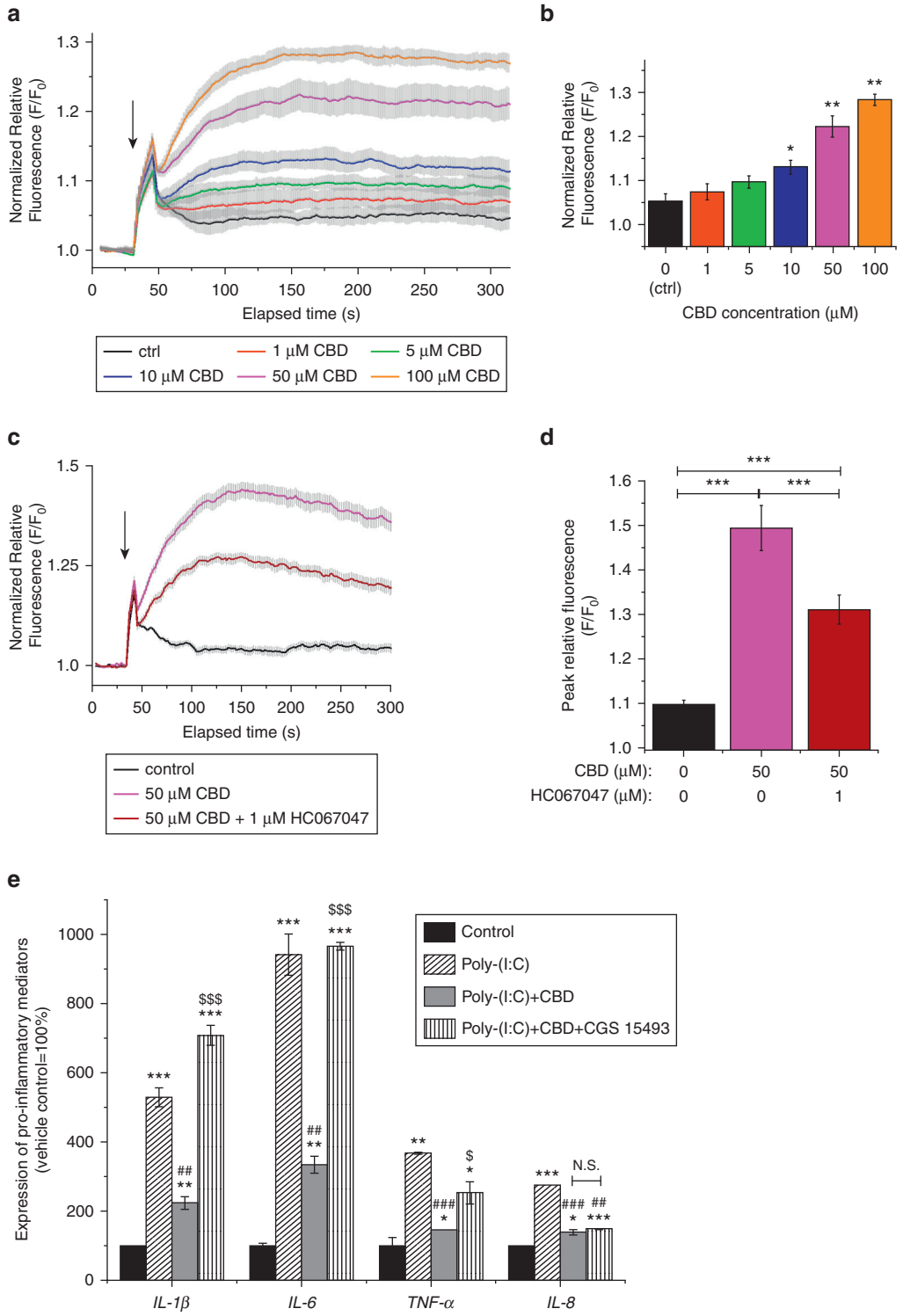

Figure 2. Procatagen concentrations of CBD activate TRPV4 ion channels, whereas at submicromolar concentration it exerts anti-inflammatory actions via the activation of adenosine receptors. (**a**–**d**) Fluo-4 AM–based fluorescent calcium measurements and their statistical analyses. Compounds were applied as indicated by the respective arrows. (**a, c**) Fluorescence (measured in relative fluorescence units) was normalized to the baseline, and is presented as mean ± standard error of the mean of F/F_0 values of N = 3–6 wells. (**b, d**) Mean ± standard error of the mean of the peak F/F_0 values measured after the indicated treatments. $^*P < 0.05$, $^{**}P < 0.01$, or $^{***}P < 0.001$, respectively, significant differences compared with (**b**) the control or (**d**) as indicated. (**e**) Quantitative real-time PCR. *TNF-α*, *IL-1β*, *IL-6*, and *IL-8* mRNA expression in human ORSKs was determined following the indicated 3-hour treatments (Poly-(I:C), 20 μg/ml; CBD, 0.1 μM; CGS 15943, 0.1 μM). Data are presented by using ΔΔCT regarding *glyceraldehyde 3-phosphate dehydrogenase*–normalized mRNA expressions of the vehicle control as 1. Data are expressed as mean ± standard deviation of three determinations. Two additional experiments yielded similar results. $^{*/\$}P < 0.05$, $^{**/\#\#}P < 0.01$, or $^{***/\#\#\#/\$\$\$}P < 0.001$, respectively (*vs. control; $^{\#}$vs. Poly-(I:C); $^{\$}$vs. Poly-(I:C) + CBD). CBD, (−)-cannabidiol; CGS 15943, a pan-antagonist of the adenosine receptors; F/F_0, normalized relative fluorescence; HC067047, specific TRPV4 antagonist; N.S., not significant; ORSK, outer root sheath keratinocyte; Poly(I:C), polyinosinic-polycytidylic acid (toll-like receptor 3 activator); TNF-α, tumor necrosis factor-α.

Oláh et al., 2017), we also assessed how a noncytotoxic (Supplementary Figures S2a-d and S3a and b) and noncatagen-promoting (Figure 1a-e) CBD concentration (i.e., 0.1 μM) impacts on the production of catagen-promoting cytokines by ORSKs. Interestingly, CBD effectively antagonized not only the toll-like receptor 3-activator polyinosinic-polycytidylic acid-induced upregulation of IL-1β, but also that of IL-6, IL-8, and tumor necrosis factor-α (Figure 2e). Similar to sebocytes, these anti-inflammatory actions of CBD appear to primarily depend on adenosine receptor-mediated signaling, because the adenosine receptor pan-antagonist CGS 15943 (Ghai et al., 1987; Klotz, 2000; Williams et al., 1987) almost completely abrogated the CBD effects reported above (Figure 2e). Besides potentially reducing the hair growth-inhibitory effects of the likely high level of these wounding-associated cytokines of freshly microdissected HFs compared with vehicle-treated controls, the moderate hair shaft-stimulatory effects of 0.1 μM CBD (Figure 1a) may also result from increased fibroblast growth factor-7 transcription by human dermal papilla fibroblasts (Iino et al., 2007). Therefore, whether submicromolar CBD helps to normalize a catagen-promoting proinflammatory HF signaling milieu, reduces the cytokine-driven recruitment and activation of hair growth inhibitory immune cells, and promotes the production of hair growth-supporting growth factors such as fibroblast growth factor-7 deserves further investigation.

Although our pilot data need to be followed up by systematic dose-response experiments in a wider range of CBD concentrations, tested in HF organ cultures from additional patients, the current data invite the hypothesis that submicromolar, adenosine receptor-activating doses of CBD may reduce the intrafollicular production of catagen-promoting cytokines and could thus become useful as adjunct therapy for inflammatory hair loss disorders characterized by excessive levels of these cytokines. Instead, TRPV4-activating micromolar concentrations of CBD are attractive candidate inhibitors of unwanted hair growth (Supplementary Figure S4). If the current ex vivo findings, which imitate a systemic mode of CBD application, are reproducible after topical application, and if administering submicromolar versus micromolar topical CBD can indeed evoke differential, therapeutically desired effects in clinical hair growth management, these results deserve rigorous exploration. Detailed discussion about the limitations of this study can be found in Supplementary Discussion.

Data avalability statement

The data that support the findings of this study are available from the corresponding authors upon reasonable request.

ORCIDs

Imre Lőrinc Szabó: https://orcid.org/0000-0002-9628-4372
Erika Herczeg-Lisztes: https://orcid.org/0000-0002-8517-6536
Gabriella Béke: https://orcid.org/0000-0003-3113-2287
Kinga Fanni Tóth: https://orcid.org/0000-0002-5184-8082
Ralf Paus: https://orcid.org/0000-0002-3492-9358
Attila Oláh: https://orcid.org/0000-0003-4122-5639
Tamás Bíró: https://orcid.org/0000-0002-3770-6221

CONFLICT OF INTEREST

AO and TB provide consultancy services to Botanix Pharmaceuticals Ltd (AO) and Phytecs Inc (TB). Botanix Pharmaceuticals Ltd, Phytecs Inc, and the founding sponsors listed in the Acknowledgments section had no role in conceiving the study, designing the experiments, writing of the manuscript, or in the decision to publish it.

ACKNOWLEDGMENTS

This project was supported by Hungarian research grants (NKFIH 120552, 121360, and 125055; GINOP-2.3.2-15-2016-00015 "I-KOM Teaming"), and has received funding from the EU's Horizon 2020 research and innovation program under grant agreement no. 739593. AO's work was supported by the János Bolyai Research Scholarship of the Hungarian Academy of Sciences and by the New National Excellence Program of the Ministry of Human Capacities (ÚNKP-18-4-DE-247). KFT's work was supported by the Hungarian Ministry of Human Capacities (NTP-NFTÖ-18-B-0168). The authors are grateful to Dániel Bereczki and to Erika Hollósi for their technical support.

AUTHOR CONTRIBUTIONS

Conceptualization: RP, AO, TB; Formal Analysis: ILS, EL; Funding Acquisition: AO, TB; Investigation: ILS, EL, GB, KFT; Project Administration: ILS, EL, GB, KFT; Supervision: AO, TB; Validation: ILS, EL; Visualization: ILS, EL; Writing - Original Draft Preparation: ILS, AO; Writing - Review and Editing: ILS, EL, GB, KFT, RP, AO, TB.

Imre L. Szabó[1,7], Erika Lisztes[1,7], Gabriella Béke[2], Kinga Fanni Tóth[1], Ralf Paus[3,4], Attila Oláh[1,7,8,*] and Tamás Bíró[5,6,7,8,*]

[1]Department of Physiology, Faculty of Medicine, University of Debrecen, Debrecen, Hungary; [2]Department of Dermatology, Faculty of Medicine, University of Debrecen, Debrecen, Hungary; [3]Centre for Dermatology Research, University of Manchester, MAHSC and NIHR Manchester Biomedical Research Centre, Manchester, United Kingdom; [4]Dr Phillip Frost Department of Dermatology & Cutaneous Surgery, University of Miami Miller School of Medicine, Miami, Florida, USA; [5]Department of Immunology, Faculty of Medicine, University of Debrecen, Debrecen, Hungary; and [6]Hungarian Center of Excellence for Molecular Medicine, Szeged, Hungary
[7]These authors contributed equally as first authors.
[8]These authors contributed equally as senior authors.
[*]Corresponding authors. e-mail: olah.attila@med.unideb.hu; biro.tamas@med.unideb.hu

SUPPLEMENTARY MATERIAL

Supplementary material is linked to the online version of the paper at www.jidonline.org, and at https://doi.org/10.1016/j.jid.2019.07.690.

REFERENCES

Armstrong JL, Hill DS, McKee CS, Hernandez-Tiedra S, Lorente M, Lopez-Valero I, et al. Exploiting cannabinoid-induced cytotoxic autophagy to drive melanoma cell death. J Invest Dermatol 2015;135:1629–37.

Chelliah MP, Zinn Z, Khuu P, Teng JMC. Self-initiated use of topical cannabidiol oil for epidermolysis bullosa. Pediatr Dermatol 2018;35:e224–7.

Crippa JA, Guimarães FS, Campos AC, Zuardi AW. Translational investigation of the therapeutic potential of cannabidiol (CBD): toward a new age. Front Immunol 2018;9:2009.

Esposito G, Filippis DD, Cirillo C, Iuvone T, Capoccia E, Scuderi C, et al. Cannabidiol in inflammatory bowel diseases: a brief overview. Phytother Res 2013;27:633–6.

Everaerts W, Zhen X, Ghosh D, Vriens J, Gevaert T, Gilbert JP, et al. Inhibition of the cation channel TRPV4 improves bladder function in mice and rats with cyclophosphamide-induced cystitis. Proc Natl Acad Sci USA 2010;107:19084–9.

Ghai G, Francis JE, Williams M, Dotson RA, Hopkins MF, Cote DT, et al. Pharmacological characterization of CGS 15943A: a novel non-xanthine adenosine antagonist. J Pharmacol Exp Ther 1987;242:784–90.

Hoffmann R, Happle R, Paus R. Elements of the interleukin-1 signaling system show hair cycle-dependent gene expression in murine skin. Eur J Dermatol 1998;8:475–7.

Iino M, Ehama R, Nakazawa Y, Iwabuchi T, Ogo M, Tajima M, et al. Adenosine stimulates fibroblast growth factor-7 gene expression via adenosine A2b receptor signaling in dermal papilla cells. J Invest Dermatol 2007;127:1318–25.

Klotz KN. Adenosine receptors and their ligands. Naunyn Schmiedebergs Arch Pharmacol 2000;362:382–91.

Langan EA, Philpott MP, Kloepper JE, Paus R. Human hair follicle organ culture: theory,

application and perspectives. Exp Dermatol 2015;24:903–11.

Maccarrone M, Bab I, Bíró T, Cabral GA, Dey SK, Di Marzo V, et al. Endocannabinoid signaling at the periphery: 50 years after THC. Trends Pharmacol Sci 2015;36:277–96.

Oh JW, Kloepper J, Langan EA, Kim Y, Yeo J, Kim MJ, et al. A guide to studying human hair follicle cycling in vivo. J Invest Dermatol 2016;136:34–44.

Oláh A, Bíró T. Targeting cutaneous Cannabinoid Signaling in Inflammation - A "High"-way to Heal? EBioMedicine 2017;16:3–5.

Oláh A, Szekanecz Z, Bíró T. Targeting Cannabinoid Signaling in the Immune System: "High"-ly Exciting Questions, Possibilities, and Challenges. Front Immunol 2017;8:1487.

Oláh A, Tóth BI, Borbíró I, Sugawara K, Szöllősi AG, Czifra G, et al. Cannabidiol exerts sebostatic and antiinflammatory effects on human sebocytes. J Clin Invest 2014;124:3713–24.

Oura H, Iino M, Nakazawa Y, Tajima M, Ideta R, Nakaya Y, et al. Adenosine increases anagen hair growth and thick hairs in Japanese women with female pattern hair loss: a pilot, double-blind, randomized, placebo-controlled trial. J Dermatol 2008;35:763–7.

Paus R, Cotsarelis G. The biology of hair follicles. N Engl J Med 1999;341:491–7.

Paus R, Langan EA, Vidali S, Ramot Y, Andersen B. Neuroendocrinology of the hair follicle: principles and clinical perspectives. Trends Mol Med 2014;20:559–70.

Pertwee RG. The diverse CB1 and CB2 receptor pharmacology of three plant cannabinoids: delta 9-tetrahydrocannabinol, cannabidiol and delta 9-tetrahydrocannabivarin. Br J Pharmacol 2008;153:199–215.

Philpott MP, Sanders DA, Bowen J, Kealey T. Effects of interleukins, colony-stimulating factor and tumour necrosis factor on human hair follicle growth in vitro: a possible role for interleukin-1 and tumour necrosis factor-alpha in alopecia areata. Br J Dermatol 1996;135:942–8.

Pisanti S, Malfitano AM, Ciaglia E, Lamberti A, Ranieri R, Cuomo G, et al. Cannabidiol: state of the art and new challenges for therapeutic applications. Pharmacol Ther 2017;175:133–50.

Ramot Y, Alam M, Oláh A, Bíró T, Ponce L, Chéret J, et al. Peroxisome proliferator-activated receptor-γ-mediated signaling regulates mitochondrial energy metabolism in human hair follicle epithelium. J Invest Dermatol 2018;138:1656–9.

Rückert R, Lindner G, Bulfone-Paus S, Paus R. High-dose proinflammatory cytokines induce apoptosis of hair bulb keratinocytes in vivo. Br J Dermatol 2000;143:1036–9.

Shin JM, Choi DK, Sohn KC, Kim SY, Min Ha J, Ho Lee Y, et al. Double-stranded RNA induces inflammation via the NF-κB pathway and inflammasome activation in the outer root sheath cells of hair follicles. Sci Rep 2017;7:44127.

Szabó IL, Herczeg-Lisztes E, Szegedi A, Nemes B, Paus R, Bíró T, et al. TRPV4 is expressed in human hair follicles and inhibits hair growth in vitro. J Invest Dermatol 2019;139:1385–8.

Telek A, Bíró T, Bodó E, Tóth BI, Borbíró I, Kunos G, et al. Inhibition of human hair follicle growth by endo- and exocannabinoids. FASEB J 2007;21:3534–41.

Tóth KF, Ádám D, Bíró T, Oláh A. Cannabinoid Signaling in the Skin: therapeutic Potential of the "C(ut)annabinoid" System. Molecules 2019;24:E918.

Williams M, Francis J, Ghai G, Braunwalder A, Psychoyos S, Stone GA, et al. Biochemical characterization of the triazoloquinazoline, CGS 15943, a novel, non-xanthine adenosine antagonist. J Pharmacol Exp Ther 1987;241:415–20.

First Glimpse of Epigenetic Effects on Pemphigus Foliaceus

Journal of Investigative Dermatology (2020) **140,** 488–491; doi:10.1016/j.jid.2019.07.691

TO THE EDITOR

Pemphigus foliaceus (PF) is an autoimmune disease, sporadic across the globe, but endemic in Brazil. A significant portion of PF autoantibodies target desmosomal glycoproteins, especially desmoglein-1, which are associated with the occurrence of painful blisters in the granular skin layer (Spindler et al., 2007). Epigenetic mechanisms have been implicated in autoimmune skin diseases. Among them, dysregulated DNA and histone methylation contribute to systemic lupus erythematosus (Hung et al., 2018), psoriasis (Manczinger and Kemény, 2013), pemphigus vulgaris (Zhao et al., 2012a), and alopecia areata (Zhao et al., 2012b). To investigate the association of genetic polymorphisms in the alteration of these mechanisms in PF, we compared 229 patients to 194 controls (52% women, median age of 43 years old, unrelated, predominantly euro-descendent, and from rural areas), genotyped with microarray hybridization (CoreExome-24, version 1.1, Illumina, San Diego, CA). The Brazilian National Ethics in Research Commission approved the protocol (02727412.4.0000.0096), and all participants gave written informed consent, according to the Declaration of Helsinki. From 1984 to 2015, individuals were recruited in the South and/or Central-Western regions of Brazil, in the Hospital Adventista do Pênfigo (Campo Grande), Lar de Caridade (Uberaba), Hospital de Clínicas (Ribeirão Preto), and Hospital de Clínicas (Curitiba). All patients presented positive Nikolsky signal and sun-exposed lesions (155 localized and 74 generalized); a total of 41 presented active lesions at the moment of blood collection, 87% of the patients were anti-desmoglein-1 positive, and all patients were negative for anti-neutrophil-cytoplasmic, anti-mitochondrial, anti-liver-kidney-microsomal, and anti-gastric-parietal-cells by ELISA (Oliveira et al., 2016) or indirect immunofluorescence (Nisihara et al., 2003). A small percentage of patients and controls (0.8–2%) were low-positive and asymptomatic for anti-smooth-muscle, anti-thyroid-microsome, and anti-nuclear-antibodies (Nisihara et al., 2003).

We selected 1,793 variants in 63 genes that code for lysine methyltransferases (KMT), demethylases (KDM), DNA methyltransferases, and ten-eleven translocation demethylases. We excluded rare variants (minor allele frequencies <0.01), variants that deviated from Hardy-Weinberg equilibrium in controls ($P < 0.05$), and variants in linkage disequilibrium ($r^2 \geq 0.8$). A total of 566 polymorphisms remained and were analyzed using logistic regression with correction for two principal components using PLINK, version 1.1.9 (http://zzz.bwh.harvard.edu/plink/). Haplotypes were reconstructed for all 61 single

Abbreviations: KDM, lysine demethylases; KMT, lysine methylase; PF, pemphigus foliaceus

Accepted manuscript published online 31 July 2019; corrected proof published online 14 October 2019

SUPPLEMENTARY MATERIALS AND METHODS

Materials

(−)-Cannabidiol (CBD), the TRPV4-selective antagonist HC067047 (Armstrong et al., 2015; http://www.guidetopharmacology.org/GRAC/LigandDisplayForward?tab=biology&ligandId=4213), and the adenosine receptor pan-antagonist CGS 15943 (Ghai et al., 1987; Klotz, 2000; http://www.guidetopharmacology.org/GRAC/LigandDisplayForward?ligandId=384) were purchased from Tocris (Bristol, United Kingdom), whereas the toll-like receptor 3 activator double-stranded RNA polyinosinic-polycytidylic acid was obtained from Sigma-Aldrich (St Louis, MO). CBD was dissolved in absolute ethanol, whereas the solvent of HC067047 and CGS 15943 was DMSO. Polyinosinic-polycytidylic acid was dissolved in filtered distilled water. Control cultures were always treated with appropriate amount of vehicle(s).

Isolation and maintenance of hair folicles

Human skin samples were obtained following obtaining written informed consent from healthy individuals undergoing dermatosurgery. The study adhered to Helsinki guidelines, and was institutionally and governmentally approved by the Institutional Research Ethics Committee and the Government Office for Hajdú-Bihar County (protocol no.: DE OEC RKEB/IKEB 3724-2012; document IDs: IX-R-052/01396-2/2012, IF-12817/2015, IF-1647/2016, and IF-778-5/2017). Human anagen VI hair follicles (HFs) were isolated from skin obtained from two male (28 and 32 years old) and one female (58 years old) patients undergoing neurosurgical intervention as described previously (Borbíró et al., 2011; Langan et al., 2015; Oláh et al., 2016). Isolated HFs were cultured in William's E Medium (Invitrogen, Paisley, United Kingdom) supplemented with 2 mM L-glutamine (Invitrogen), 10 ng/ml hydrocortisone, 10 mg/ml insulin, and antibiotics (all from Sigma-Aldrich). Treatments were initiated 24 hours after the isolation. Medium was changed every other day, whereas treatment with CBD (or vehicle) was performed daily. Length measurements were performed on individual HFs using a light microscope with an eyepiece measuring graticule.

Isolation and culture of outer root sheath keratinocytes

Isolation and culture of outer root sheath keratinocytes (ORSKs) was performed following our previously optimized protocols (see, e.g., Borbíró et al., 2011; Ramot et al., 2018). In brief, plucked hair shafts of healthy volunteers (both females and males; aged 23−47 years old) were digested using trypsin to isolate ORSKs. Isolated ORSKs were seeded to a feeder layer of primary human dermal fibroblasts that were pretreated overnight with mitomycin C (0.4 μg/ml from Sigma-Aldrich) to block their proliferation. Human dermal fibroblasts were obtained from de-epidermized dermis using enzymatic digestion. Cocultures of nonproliferating feeder human dermal fibroblasts and ORSKs were maintained in a 1:3 mixture of Ham's F-12 and DMEM (both from Invitrogen) supplemented with 0.1 nM cholera toxin, 5 mg/ml insulin, 0.4 mg/ml hydrocortisone, 2.43 mg/ml adenine, 2 nM triiodothyronine, 10 ng/ml EGF, 1 mM ascorbyl-2-phosphate, and antibiotics (all from Sigma-Aldrich). ORSKs were plated for subsequent experiments on collagen-coated (1%; 37 °C for 1 hour; obtained from Sigma-Aldrich) culture dishes without human dermal fibroblast feeder layer.

Hematoxylin and eosin staining of frozen tissue sections

Cryosections of 6 μm thickness of the HFs were dried at room temperature (10 minutes), and fixed in precooled acetone (10 minutes at −20 °C). Sections were then washed in distilled water for 1 minute at room temperature, and stained with Mayer's hematoxylin for 35 seconds at room temperature. Following gentle washing under the tap water for 15 minutes at room temperature, sections were stained with 0.1% Eosin Y solution (1 minute at room temperature). Sections were then dehydrated (washing three to four times in 70%, 96%, and 100% ethanol), and incubated in xylene (2 × 10 minutes at room temperature). Finally, sections were mounted by using Eukitt quick-hardening mounting medium (Sigma-Aldrich). Images were taken by using bright-field function of a Nikon Eclipse E600 microscope (Nikon, Tokyo, Japan). Hematoxylin and eosin staining was then used for studying HF morphology, and, together with Ki-67/TUNEL double labeling , for staging hair cycle to anagen, early catagen, and late catagen according to predefined objective morphological criteria (Kloepper et al., 2010).

Assessment of proliferation and apoptosis of matrix keratinocytes (Ki-67/TUNEL double labeling)

Proliferation and apoptosis were assessed by Ki-67/TUNEL double immunostaining as described previously (Borbíró et al., 2011; Kloepper et al., 2010; Oláh et al., 2016). In brief, cryosections (6 μm) were air dried for 10 minutes at room temperature, and then fixed for 10 minutes in 1% paraformaldehyde in phosphate-buffered saline (PBS) (15 mM NaCl, 20 mM Na_2HPO_4 [pH 7.4]; all from Sigma-Aldrich) at room temperature. Samples were rehydrated in PBS for 5 minutes (2×), and were then postfixed for 5 minutes in precooled ethanol−acetic acid 2:1 at −20 °C, and then rehydrated in PBS again for 5 minutes (3×). After rehydration, sections were incubated with an equilibration buffer for 5 minutes at room temperature, and then incubated with TdT enzyme for 1 hour at 37 °C. To reveal proliferation, mouse anti-human Ki-67 (DAKO, Carpinteria, CA) primary antibody was used. In addition, to assess apoptosis, a TUNEL assay was performed using an ApopTag Fluorescein In Situ Apoptosis Detection Kit (Merck Millipore) following the manufacturer's instructions. Sections were incubated with the primary antibody overnight at 4 °C, and then with the secondary antibody (Alexa Fluor 568 Goat anti-Mouse IgG; Invitrogen) for 45 minutes at room temperature. Sections were washed in PBS and were counterstained with DAPI (Sigma-Aldrich) and mounted with Fluoromont-G (Southern Biotechnology Associates, Birmingham, AL). Visualization of the signals was performed using a Nikon Eclipse E600 fluorescent microscope (Nikon). The ratio of proliferating (Ki-67$^+$) and apoptotic (TUNEL$^+$) cells was determined in defined reference regions of the hair bulb, and are expressed as the

percentage of the total cell count determined by counting $DAPI^+$ nuclei.

Quantitative real-time PCR

Quantitative real-time PCR was performed on a Stratagene MXP3005p detection system (Agilent Technologies, Santa Clara, CA) using the 5′ nuclease assay, as we have described previously (Oláh et al., 2014). In brief, ORSKs were seeded to Petri dishes (d = 35 mm; 500,000 cells/1.5 ml medium/dish), and were harvested following the indicated 3-hour treatments. Total RNA was then isolated using TRIzol reagent (Invitrogen) according to the manufacturer's protocol. The concentrations and purities of the RNA samples were measured using a NanoDrop ND-1000 spectrophotometer (Thermo Fischer Scientific, Budapest, Hungary), and samples were kept at −20 °C until further processing. Next, DNase treatment was performed according to the manufacturer's protocol, and, then, 3 μg of total RNA was reverse-transcribed into cDNA using a High-Capacity cDNA Kit from Life Technologies Hungary, Budapest, Hungary. PCR amplification was performed using the TaqMan Gene Expression Assays (assay IDs: Hs00174097_m1 for *IL-1α*; Hs00985639_m1 for *IL-6*; Hs00174103_m1 for *IL-8*; and Hs00174128_m1 for *tumor necrosis factor-α*) and the TaqMan Universal PCR Master Mix protocol (Applied Biosystem, Waltham, MA). As internal control, transcripts of *glyceraldehyde 3-phosphate dehydrogenase* (assay ID: Hs99999905_m1) were determined. The amount of the transcripts was normalized to those of the housekeeping gene using the ΔCT method, and then the relative expression values were further normalized those of the vehicle-treated control (ΔΔCT method).

Fluorescent Calcium measurements

ORSKs were seeded in 96-well black well plates with clear bottom (Greiner Bio-One, Kremsmuenster, Austria) previously coated with 1% collagen in ORSK medium at a density of 20,000 cells per well, and incubated at 37 °C for 24 hours. The cells were washed once with 10 mg/ml BSA and 2.5 mM probenecid (both from Sigma-Aldrich) containing Hank's solution (136.8 mM NaCl, 5.4 mM KCl, 0.34 mM Na_2HPO_4, 0.44 mM KH_2PO_4, 0.81 mM $MgSO_4$, 1.26 mM $CaCl_2$, 5.56 mM glucose, 4.17 mM $NaHCO_3$ [pH 7.2], all from Sigma-Aldrich), and then were loaded with 1 μM Fluo-4 AM (Life Technologies Hungary) dissolved in Hank's solution (100 μl/well) at 37 °C for 30 minutes. The cells were then washed three times with Hank's solution (100 μl/well). The plates were then placed into a FlexStation II^{384} Multi-Mode Microplate Reader (Molecular Devices, Sunnyvale, CA) and alterations of the cytoplasmic calcium concentration (reflected by changes in fluorescence; λ_{EX} = 490 nm, λ_{EM} = 520 nm) were monitored at room temperature following the application of the indicated substances or vehicle. To probe reactivity and viability of the cells, at the end of each measurement, 0.2 mg/ml adenosine triphosphate was administered as a positive control (data not shown). Data are presented as F/F_0, where F_0 is the average baseline fluorescence (i.e., before compound application), whereas F is the actual fluorescence.

Determination of cellular proliferation

The degree of cellular growth (reflecting proliferation) was determined by measuring the DNA content of cells using a CyQUANT Cell Proliferation Assay Kit (Life Technologies Hungary). ORSKs (5,000 cells per well) were cultured in 96-well black well plates with clear bottom (Greiner Bio-One), and were treated as indicated in octuplicates. Supernatants were then removed by blotting on paper towels, and the plates were subsequently frozen at −80 °C. The plates were then thawed at room temperature, and 200 μl of CyQUANT dye/cell lysis buffer mixture was added to each well. After 5 minutes of incubation, fluorescence was measured at 490 nm excitation and 520 nm emission wavelengths using a FlexStation II^{384} Multi-Mode Microplate Reader (Molecular Devices). Relative fluorescence values were expressed as the percentage of the daily vehicle control regarded as 100%.

Evaluation of cellular viability

To assess the effect on viability, we applied an MTT assay (Sigma-Aldrich) because mitochondrial enzymes of living cells are able to transform tetrazolium salt (MTT) into formazan crystals. ORSKs were seeded in 96-well plates (density: 10,000 cells/well) and were treated as indicated in octuplicates with various concentrations of CBD or vehicle. Cells were then incubated with 0.5 mg/ml MTT reagent for 3 hours, and the concentration of formazan crystals (as an indicator of number of viable cells) was determined colorimetrically at 565 nm by using a FlexStation 3 Multi-Mode Microplate Reader (Molecular Devices). Results are expressed as percentage of vehicle control regarded as 100%.

Determination of apoptosis

A decrease in the mitochondrial membrane potential is one of the earliest markers of apoptosis (Green and Reed, 1998; Susin et al., 1998). Therefore, to assess the process, the mitochondrial membrane potential of ORSKs was determined using a MitoProbe $DilC_1(5)$ Assay Kit (Life Technologies Hungary). Cells (10,000 cells/well) were cultured in 96-well black well plates with clear bottom (Greiner Bio-One) in octuplicates and were treated as indicated. After removal of supernatants, cells were incubated for 30 minutes with $DilC_1(5)$ working solution (50 μl/well), then washed with PBS, and the fluorescence of $DilC_1(5)$ was measured at 630 nm excitation and 670 nm emission wavelengths using a FlexStation II^{384} Multi-Mode Microplate Reader (Molecular Devices). Relative fluorescence values were expressed as the percentage of vehicle control regarded as 100%.

Determination of necrosis

Necrotic processes were determined by SYTOX Green staining (Life Technologies Hungary). The dye is able to penetrate (and then to bind to the nucleic acids) only necrotic cells with ruptured plasma membranes, whereas healthy cells with intact surface membranes show negligible SYTOX Green staining intensity. Cells were cultured in 96-well black well plates with clear bottom (Greiner Bio-One), and treated as indicated. Supernatants were then discarded, and the cells were incubated for 30 minutes with 1 μM SYTOX Green dye. Following incubation, cells were washed with PBS, the culture medium

was replaced, and fluorescence of SYTOX Green was measured at 490 nm excitation and 520 nm emission wavelengths using a FlexStation II^{384} Multi-Mode Microplate Reader (Molecular Devices). Relative fluorescence values were expressed as the percentage of negative control regarded as 100%. Owing to their spectral properties, $DiIC_1(5)$ and SYTOX Green dyes were always administered together, enabling us to investigate necrotic and early apoptotic processes of the same cultures. Selective decrease of $DiIC_1(5)$ intensity indicated mitochondrial depolarization (i.e., the onset of early apoptotic processes), whereas increase of SYTOX Green staining intensity revealed necrotic cell death.

Statistical analysis

When applicable, data were analyzed using OriginPro Plus 6 software (Microcal, Northampton, MA) using chi-square test followed by Fisher's exact test, Student two-tailed unpaired *t*-test, or analysis of variance with Bonferroni post hoc test, and $P < 0.05$ values were regarded as significant differences.

SUPPLEMENTARY DISCUSSION

Limitations of this Study

When interpreting the results presented in the current exploratory, pilot study, one has to keep in mind that, although it sheds light on previously unknown and potentially relevant (hair-wise) dermatological effects of CBD, the current work has certain important limitations as well.

First and foremost, as mentioned in the main text, our data need to be followed up by systematic dose-response experiments in a wider range of CBD concentrations, tested in HF organ cultures from additional patients to explore the existence and magnitude of inter-donor variability.

Second, in the current study, by adding CBD (or vehicle) to the culture medium we mimicked the effects of systematically administered CBD. However, from a translational point-of-view it is crucially important to assess the biological effects of CBD following standardized topical application in appropriate formulations.

Third, it is important to emphasize that, in the current study, we used microdissected, truncated HFs lacking the bulge region as well as other (non-HF) members of the pilosebaceous unit (namely the sebaceous glands and the arrector pili muscles). Therefore, we cannot exclude the possibility that specific (and most likely concentration dependent) actions of CBD on these structures may influence the production and release of hair cycle-regulating substances, further modifying its already quite complex effects on the hair cycle.

Fourth, studying microdissected HFs ex vivo has the inherent limitation of missing the effects and regulatory roles of intact innervation and blood supply. This may be crucially important, because it can lead to model dependently opposing observations in certain cases. In the case of, for example, the TRPV1-activating capsaicin, we have previously shown that it suppressed hair growth and induced premature catagen entry in microdissected human HFs (Bíró et al., 2006). Moreover, lack of TRPV1 in knockout animals delayed their normal hair cycle (Bodó et al., 2005). However, administration of capsaicin was found to promote hair growth by increasing IGF-I production in mice and in humans with alopecia, most likely by acting on sensory nerve fibers (Harada et al., 2007). Given the broad target spectrum of CBD, one can speculate that it may also modulate production and release of hair cycle-regulating substances from sensory nerve endings. Therefore, its impact on human hair biology may be even more complex.

SUPPLEMENTARY REFERENCES

Armstrong JL, Hill DS, McKee CS, Hernandez-Tiedra S, Lorente M, Lopez-Valero I, et al. Exploiting cannabinoid-induced cytotoxic autophagy to drive melanoma cell death. J Invest Dermatol 2015;135:1629–37.

Bíró T, Bodó E, Telek A, Géczy T, Tychsen B, Kovács L, et al. Hair cycle control by vanilloid receptor-1 (TRPV1): evidence from TRPV1 knockout mice. J Invest Dermatol 2006;126:1909–12.

Bodó E, Bíró T, Telek A, Czifra G, Griger Z, Tóth BI, et al. A hot new twist to hair biology: involvement of vanilloid receptor-1 (VR1/TRPV1) signaling in human hair growth control. Am J Pathol 2005;166:985–98.

Borbíró I, Lisztes E, Tóth BI, Czifra G, Oláh A, Szöllosi AG, et al. Activation of transient receptor potential vanilloid-3 inhibits human hair growth. J Invest Dermatol 2011;131:1605–14.

Esposito G, Filippis DD, Cirillo C, Iuvone T, Capoccia E, Scuderi C, et al. Cannabidiol in inflammatory bowel diseases: a brief overview. Phytother Res 2013;27:633–6.

Ghai G, Francis JE, Williams M, Dotson RA, Hopkins MF, Cote DT, et al. Pharmacological characterization of CGS 15943A: a novel non-xanthine adenosine antagonist. J Pharmacol Exp Ther 1987;242:784–90.

Green DR, Reed JC. Mitochondria and apoptosis. Science 1998;281:1309–12.

Harada N, Okajima K, Arai M, Kurihara H, Nakagata N. Administration of capsaicin and isoflavone promotes hair growth by increasing insulin-like growth factor-I production in mice and in humans with alopecia. Growth Horm IGF Res 2007;17:408–15.

Iino M, Ehama R, Nakazawa Y, Iwabuchi T, Ogo M, Tajima M, et al. Adenosine stimulates fibroblast growth factor-7 gene expression via adenosine A2b receptor signaling in dermal papilla cells. J Invest Dermatol 2007;127:1318–25.

Kloepper JE, Sugawara K, Al-Nuaimi Y, Gáspár E, van Beek NV, Paus R. Methods in hair research: how to objectively distinguish between anagen and catagen in human hair follicle organ culture. Exp Dermatol 2010;19:305–12.

Klotz KN. Adenosine receptors and their ligands. Naunyn Schmiedebergs Arch Pharmacol 2000;362:382–91.

Langan EA, Philpott MP, Kloepper JE, Paus R. Human hair follicle organ culture: theory, application and perspectives. Exp Dermatol 2015;24:903–11.

Oláh A, Gherardini J, Bertolini M, Chéret J, Ponce L, Kloepper J, et al. The thyroid hormone analogue KB2115 (eprotirome) prolongs human hair growth (Anagen) ex vivo. J Invest Dermatol 2016;136:1711–4.

Oláh A, Tóth BI, Borbíró I, Sugawara K, Szöllõsi AG, Czifra G, et al. Cannabidiol exerts sebostatic and antiinflammatory effects on human sebocytes. J Clin Invest 2014;124:3713–24.

Ramot Y, Alam M, Oláh A, Bíró T, Ponce L, Chéret J, et al. Peroxisome proliferator-activated receptor-γ-mediated signaling regulates mitochondrial energy metabolism in human hair follicle epithelium. J Invest Dermatol 2018;138:1656–9.

Szabó IL, Herczeg-Lisztes E, Szegedi A, Nemes B, Paus R, Bíró T, et al. TRPV4 is expressed in human hair follicles and inhibits hair growth in vitro. J Invest Dermatol 2019;139:1385–8.

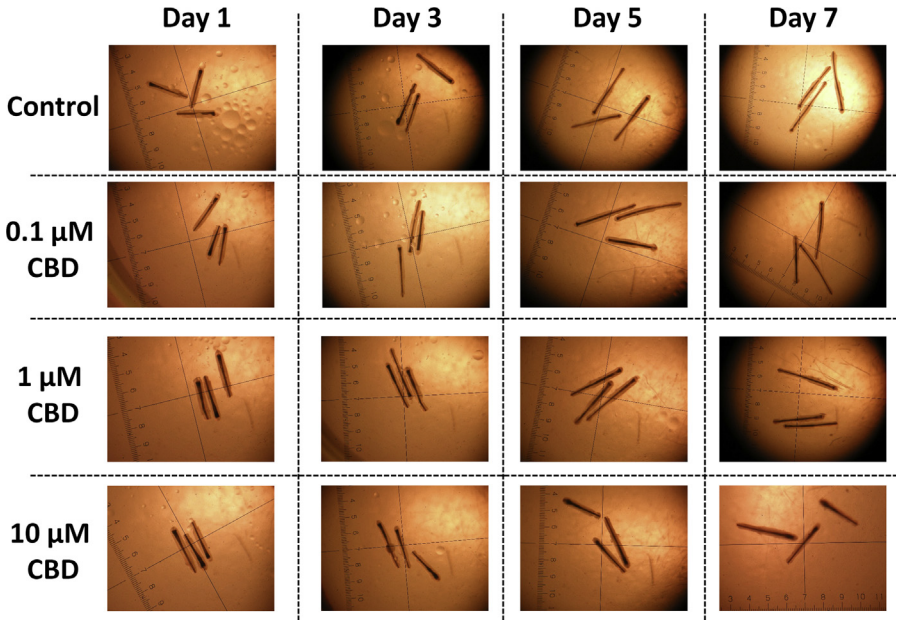

Supplementary Figure S1. Macroscopic appearance of the HFs following the indicated CBD or vehicle treatments (representative images). CBD, (−)-cannabidiol.

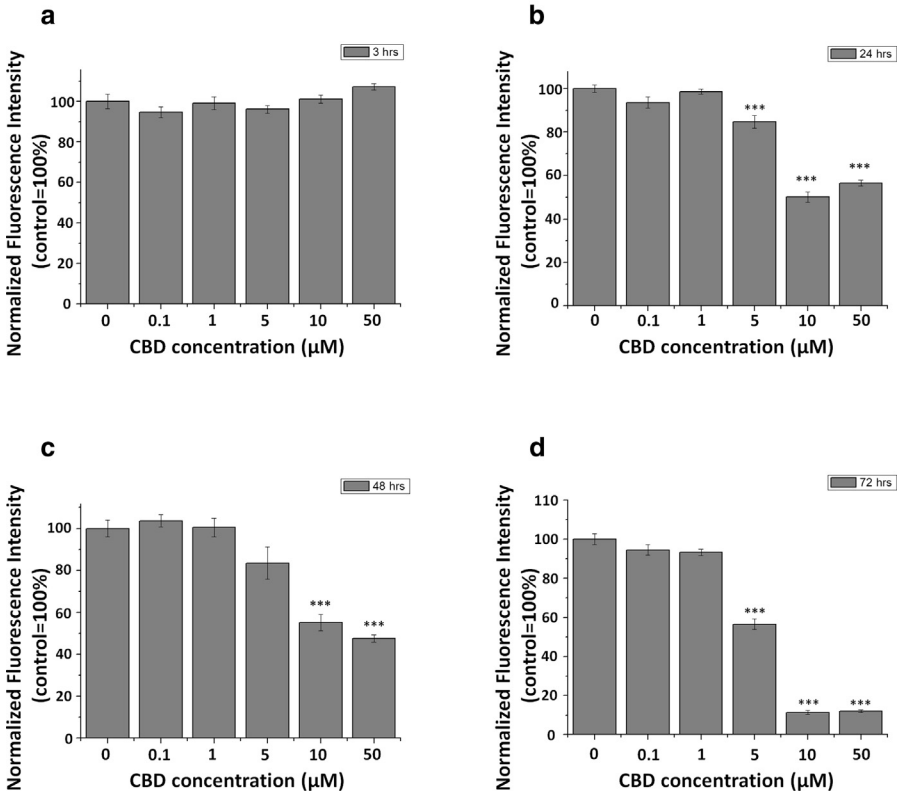

Supplementary Figure S2. CBD decreases the ORSK cell count in a concentration- and time-dependent manner. (**a**-**d**) CyQUANT assays. ORSKs were plated at low (5,000/well) initial cell count to enable rapid proliferation. Cell count was assessed following (**a**) 3-, (**b**) 24-, (**c**) 48-, and (**d**) 72-hour treatments. Results are expressed in the percentage of the daily vehicle control as mean ± standard error of the mean of eight independent determinations. Two additional experiments yielded similar results. ***$P < 0.001$ significant difference compared with the respective control group. CBD, (−)-cannabidiol; ORSK, outer root sheath keratinocyte.

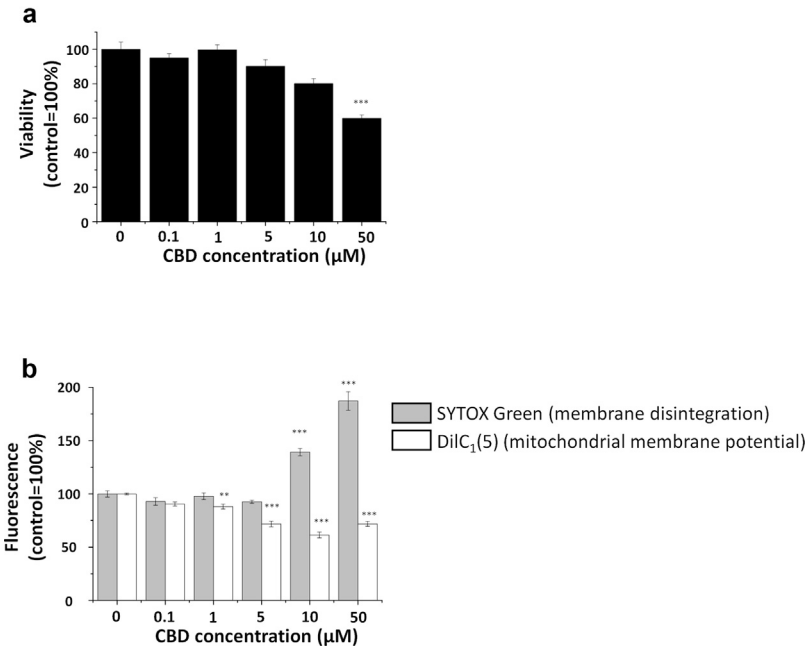

Supplementary Figure S3. High CBD concentrations reduce viability, and induce apoptosis-dominated cell death. (**a**) ORSKs were treated as indicated for 24 hours, and viability and (**b**) cell death were assessed by MTT assay and combined $DilC_1(5)$-SYTOX Green labeling, respectively. Results are expressed in the percentage of the vehicle control as mean ± standard error of the mean of eight independent determinations. Two additional experiments yielded similar results. ** $P < 0.01$ or *** $P < 0.001$, respectively, significant differences compared with the respective control group. CBD, (−)-cannabidiol; $DilC_1(5)$, 1,1′,3,3,3′,3′-hexamethylindodicarbo-cyanine iodide; ORSK, outer root sheath keratinocyte.

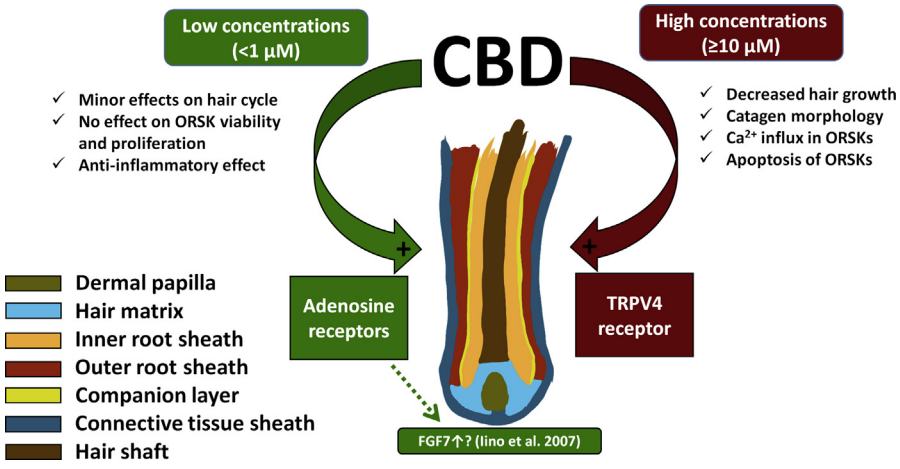

Supplementary Figure S4. Overview of the effects of CBD: CBD differentially influences human HF biology in a concentration-dependent manner. High (≥10 μM) concentrations of CBD induced premature catagen entry by activating TRPV4 ion channels expressed on the ORSKs. Importantly, such a procatagen effect of TRPV4 is not unprecedented, since it has recently been demonstrated that activation of this channel, similar to that of the structurally closely related TRPV3 (Borbíró et al., 2011) and TRPV1 (Bíró et al., 2006; Bodó et al., 2005), is a potent inducer of catagen transformation of human HFs (Szabó et al., 2019). Intriguingly, however, when applied at low, submicromolar concentrations, CBD tended to promote hair shaft production. Although, in light of the unaltered proliferation and apoptosis rates, this may represent a pseudo-elongation of the hair shaft, which is pushed out of its anchorage in the HF by tissue shrinkage during the course of organ culture, our data indicate that submicromolar concentrations of CBD may exert a differential effect on human HFs. Indeed, 0.1 μM CBD prevented the toll-like receptor 3 activator polyinosinic-polycytidylic acid-induced upregulation of several proinflammatory cytokines in cultured ORSKs in an adenosine receptor-dependent manner, since the adenosine receptor pan-antagonist CGS 15943 (0.1 μM) could almost completely abrogate this effect. Although exploration of the adenosine receptor expression profile of human HFs is beyond the scope of the current letter, these data suggest that, besides the ones expressed on the dermal papilla cells (Iino et al., 2007), adenosine receptors of the ORSKs are also functionally active, and may contribute to the regulation of hair cycle, as well as of other aspects of HF biology. Obviously, it remains to be investigated in future targeted studies if moderate hair shaft production-promoting effects of low CBD concentrations are coupled to the A_{2B} receptor-dependent upregulation of fibroblast growth factor-7 expression in the dermal papilla (Iino et al., 2007), or are rather mediated in an ORSK-dependent manner, or that the two pathways complement each other. FGF7, fibroblast growth factor-7; ORSK, outer root sheath keratinocyte.